Large-Capacity Oxygen Storage by Lanthanide Oxysulfate/Oxysulfide Systems

Masato Machida,* Kiyotaka Kawamura, Kazuhiro Ito, and Keita Ikeue

Department of Applied Chemistry and Biochemistry, Faculty of Engineering, Kumamoto University, Kumamoto 860-8555, Japan

Received November 22, 2004. Revised Manuscript Received January 20, 2005

The present work has demonstrated the large-capacity oxygen storage of various isomorphous lanthanide oxysulfates, $Ln_2O_2SO_4$ (Ln = La, Pr, Nd and Sm), which utilize the nonmetallic element (S) as a redox site instead of metallic cations. The reduction by H_2 or hydrocarbons and subsequent reoxidation by O_2 between $Ln_2O_2SO_4(S^{6+})$ and $Ln_2O_2S(S^{2-})$ achieved an oxygen storage of 2 (mol of O_2)·mol^{-1}, which is 8 times larger than that of the conventional CeO_2-ZrO_2 material. Although the reversible redox cycle of thermostable $Ln_2O_2SO_4$ with Ln = La, Sm, and Nd was possible only at high temperatures above 700 °C, the Pr system could work at an exceptionally low temperature of ca. 600 °C. Furthermore, the redox of the Pr system could be accelerated in the presence of impregnated noble metals (1 wt % Pd), which supply activated hydrogen as well as oxygen by spillover. Because the elimination of a large amount of sulfate species as SO_2/O_2 from the bulk crystallites of sulfate precursors yields the macroporous texture of $Ln_2O_2SO_4$ and Ln_2O_2S with a high specific surface area, the resultant rapid gas diffusion as well as solid−gas reactions would facilitate the oxygen storage and release processes.

Introduction

Oxygen storage capacity is the ability to store oxygen under an oxidizing atmosphere and release it under a reducing atmosphere. The role is very useful for regulating oxygen partial pressure in the gas phase. Recently, oxygen storage materials have become significantly important in the field of solid-state chemistry after being applied to the three-way automotive catalyst to compensate the fluctuation between lean (oxidizing) and rich (reducing) exhaust conditions.[1−3] Many metal oxides with a redox property are candidates for this purpose. Practically, however, the CeO_2-ZrO_2 binary system is a sole component for the automotive application due to its reversible and rapid release and sorption of oxygen at relatively low temperatures (≤400 °C).[4−8] Since the reaction is based on the redox between Ce^{4+} and Ce^{3+} and corresponding solid−gas oxygen equilibrium, the oxygen storage capacity can therefore not exceed 0.25 (mol of O_2)·mol^{-1}. The oxygen storage materials will be applied to not only automotive catalysts but also other high-temperature processes, where instant oxygen scavengers are required. Possible processes may include nonaerobic oxidation processes and H_2-O_2 fuel cells,[9,10] which can be improved by incorporating the oxygen storage material into a cathode. To open up such new applications of the oxygen storage, new materials with larger storage capacity per unit of solid volume are strongly requested.

We have recently found a novel oxygen storage mechanism based on the redox of sulfur in a lanthanum oxysulfate/oxysulfide ($La_2O_2SO_4/La_2O_2S$) system,[11] which is the first successful example that uses a nonmetallic element as a redox site in place of metallic cations. On the basis of the following redox reaction between S^{6+} and S^{2-}

$$Ln_2O_2SO_4 \rightleftarrows Ln_2O_2S + 2O_2$$

the storage capacity of 2 mol·mol^{-1} is possible, which is the largest value reported so far. Nevertheless, the higher operation temperature of ≤700 °C becomes a major drawback of the present system, compared to ≤400 °C, which enough for CeO_2-ZrO_2. Modifications to reduce the redox temperature are strongly requested for the practical application. One possible modification is to replace La by other lanthanide elements; i.e., a series of the isomorphous lanthanide (Ln) oxysulfate phases are reported,[12−14] which are the subject of considerable interest because their oxygen storage property has not been studied so far. The purpose of

* To whom correspondence should be addressed. Phone/fax: +81-96-342-3651. E-mail: machida@chem.kumamoto-u.ac.jp.

(1) Taylar, K. C. Automobile catalytic converters. In *Catalysis-Science and Technology*; Anderson, J. R., Boudart, M., Eds.; Springer-Verlag: Berlin, 1984; Vol. 5.
(2) Bernal, S.; Kaspar, J.; Trovarelli, A. *Catal. Today* **1999**, *2*, 50.
(3) Trovarelli, A. In *Catalysis by ceria and related materials*; Trovarelli, A., Ed.; Imperial College Press: London, 2002; Vol. 2.
(4) Ozawa, M.; Kimura, M.; Isogai, A. *J. Alloys Compd.* **1993**, *193*, 73.
(5) Zamur, F.; Trovarelli, A.; de Leitenburg, C.; Dolcetti, G. *J. Chem. Soc., Chem. Commun.* **1995**, 965.
(6) Balducci, G.; Fornasiero, P.; Di Monte, R.; Kaspar, J.; Meriani, S.; Graziani, M. *Catal. Lett.* **1995**, *33*, 193.
(7) Kaspar, J.; Fornasiero, P. *J. Solid State Chem.* **2003**, *171*, 19.
(8) Pijolat, M.; Prin, M.; Soustelle, M.; Touret, O.; Nortier, P. *J. Chem. Soc., Faraday Trans.* **1995**, *91*, 3941.
(9) Sakakini, B. H.; Taufiq-Yap, Y. H.; Waugh, K. C. *J. Catal.* **2000**, *189*, 253.
(10) Xu, Z.; Qi, Z.; Kaufman, A. *J. Power Sources* **2003**, *115*, 40.
(11) Machida, M.; Kawamura, K.; Ito, K. *Chem. Commun.* **2004**, 662.
(12) Clark, T. E.; Burilla, C. T. *J. Electrochem. Soc.* **1982**, *129*, 1540.
(13) Porcher, P.; Svoronos, D. R.; Leskela, M.; Holsa, J. *J. Solid State Chem.* **1983**, *46*, 101.
(14) Zhukov, S.; Yatsenko, A.; Chernyshev, V.; Trunov, V.; Tserkovnaya, E.; Anston, O.; Hosla, J.; Baules, P.; Schenk, H. *Mater. Res. Bull.* **1997**, *32*, 43.

10.1021/cm0479640 CCC: $30.25
Published on Web 02/26/2005

the present work is to synthesize a series of lanthanide oxysulfates ($Ln_2O_2SO_4$, Ln = La, Pr, Nd, Sm, Eu, Y, Tb, and Gd) and characterize their thermal stability and redox property to use them as large-capacity oxygen storage materials. The effects of different Ln and noble metal impregnations on the redox property have been examined by means of X-ray diffraction, temperature-programmed reduction/reoxidation, thermogravimetry, and microstructure analysis.

Experimental Section

A series of lanthanum oxysulfates, $Ln_2O_2SO_4$, were synthesized by heating commercial $Ln_2(SO_4)_3 \cdot nH_2O$ (Ln = Y, La, Pr, Nd, Sm, Eu, Gd, and Tb; Rare Metallic Co., Ltd.) at 900 °C for 5 h in a stream of N_2 or air. Subsequent heating in a stream of H_2 at 800 °C was conducted to yield corresponding oxysulfides, Ln_2O_2S. As a reference, the binary solid solution of CeO_2-ZrO_2 was synthesized[15,16] and used to evaluate the cyclic oxygen release and storage properties. The samples thus obtained were impregnated with an aqueous solution of hydrogen hexachloroplatinate(IV) or palladium nitrate and then calcined at 450 °C to produce Pt- or Pd-loaded samples (1 wt % loading). The crystal structure was identified by use of a powder X-ray diffractometer (Rigaku Multiflex) with monochromated Cu Kα radiation (30 kV, 20 mA). Energy-dispersive X-ray fluorescence analysis (Horiba MESA-500W) was used to determine the S/Ln ratio. The thermal decomposition of lanthanide sulfates was studied by thermogravimetric (TG) analysis (Rigaku 8120). The surface microstructure of as-formed samples was observed by FE-SEM (Hitachi S-4100). The BET surface area and pore size distribution were calculated from N_2 adsorption isotherms measured at 77 K (Belsorp).

The reduction/reoxidation behavior of $Ln_2O_2SO_4$ was analyzed by temperature-programmed reduction and reoxidation (TPR/TPRO) in a conventional flow reactor connected to a volumetric vacuum system and to a differential evacuation system. After evacuation at ambient temperature, the sample (0.2 g) was heated in a flowing gas mixture of 10% H_2 and He or 1% C_3H_6 and He (20 $cm^3 \cdot min^{-1}$) at a constant rate (10 °C·min^{-1}) up to 950 °C. Effluent gas from the sample was analyzed by a quadrupole residual gas analyzer−mass spectrometer (Anelva M100). After the TPR measurement was completed, the sample was cooled slowly to ambient temperature in a stream of 5% H_2/He. This was followed by evacuation and the second heating in a flowing gas mixture of 5% O_2/He (20 $cm^3 \cdot min^{-1}$) at a constant rate (10 °C·min^{-1}) up to 950 °C to measure the TPRO profiles.

Dynamic reduction−oxidation cycles of $Ln_2O_2SO_4$ were studied by the use of a microbalance (TG, Rigaku 8120), which is connected to a dual-gas-supplying system. The oxysulfate sample (ca. 10 mg) was first heated in a stream of N_2 up to 700 °C, where the constant weight was attained within 30 min. Then, the gas feed to sample was switched between 5% H_2 and 20% O_2 balanced by N_2 with recording of the sample weight at this temperature. During the measurement, N_2 flowed through the balance chamber to protect the weighing mechanism.

Results and Discussion

A single phase of lanthanum oxysulfate, $La_2O_2SO_4$, could be synthesized by heating $La_2(SO_4)_3 \cdot 9H_2O$ powders at 900 °C for 5 h in N_2 or air. But further decomposition could not be accomplished even after heating at 1100 °C. The thermal decomposition of several lanthanide sulfates ($Ln_2(SO_4)_3 \cdot nH_2O$, Ln = La, Pr, Nd, Sm, Eu, Gd, and Tb) in flowing N_2 was studied by TG analysis. The TG curves yielded two independent weight losses after dehydration at ≥300 °C, which correspond to the following two reactions:

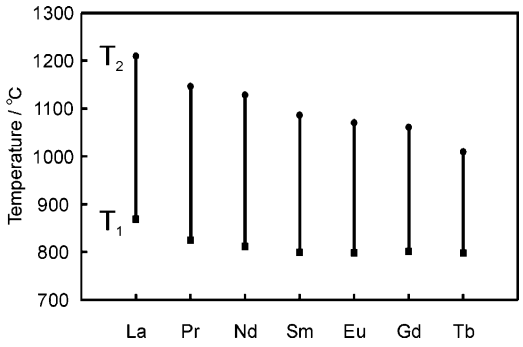

Figure 1. Temperature of decomposition of $Ln_2(SO_4)_3$ and $Ln_2O_2SO_4$ in a flow of N_2.

$$Ln_2(SO_4)_3 \xrightarrow{T_1} Ln_2O_2SO_4 + 2SO_2 + O_2$$

$$Ln_2O_2SO_4 \xrightarrow{T_2} Ln_2O_3 + SO_2 + {}^1/_2O_2$$

Here, the temperatures T_1 and T_2 were determined from a peak minimum of a differential TG curve and plotted against Ln in Figure 1. All these lanthanides exhibited a similar decomposition behavior, but both T_1 and T_2 tend to decrease monotonically with increasing atomic number. Since T_2 is more dependent on the atomic number in contrast to T_1, the resultant stability range of oxysulfate phases is found to be widest for Ln = La. Yttrium also forms an oxysulfate, $Y_2O_2SO_4$, which is decomposed to Y_2O_3 at ca. 950 °C. The decrease of the thermal stability of sulfate and oxysulfate is associated with the thermodynamic stability of Ln_2O_3, which increases with the atomic number because the lanthanide contraction yields a larger heat of formation ($-\Delta H_f°$) of the oxides with a similar crystal structure. The only exception is the sulfate of Ce^{4+}, which eliminates all of the sulfate species as SO_2/O_2 at <700 °C to produce CeO_2. Considering the instability of $Ln_2O_2SO_4$ above 1100 °C, the lanthanides heavier than Sm should be limited for practical applications. The following study has therefore been focused on the oxysulfates of the first four lanthanides (La, Pr, Nd, and Sm) to evaluate their reduction/reoxidation behavior.

Figure 2 shows the XRD patterns taken after Ln sulfates were heated in a stream of N_2 at 900 °C. Clearly, $Ln_2O_2SO_4$ phases were obtained without precipitation of impurities. For Ln = La, the observed peaks could be attributed to a monoclinic $La_2O_2SO_4$ (*C*2/*c*) with lattice dimensions of a = 1.4349 nm, b = 0.4285 nm, c = 0.8386 nm, and $\beta = 107°$.[14] Although the structural analysis of the other Ln phases has not been reported, all the reflections indexed with the *C*2/*c* space group suggested that their crystal structures are basically the same as that of the La system. The estimated lattice parameters *a*, *b*, and *c* decreasing with an increase of atomic number is consistent with the contraction of Ln^{3+}. Figure 3 shows the XRD patterns taken after reduction of

(15) Ohmata, T.; Kishimoto, H.; Matsumo, S.; Ohtori, N.; Umesaki, N. *J. Solid State Chem.* **1999**, *147*, 573.
(16) Tanabe, T.; Suda, A.; Descorme, C.; Duprez, D.; Shinjodh, H.; Sugiura, M. *Stud. Surf. Sci. Catal.* **2001**, *138*, 135.

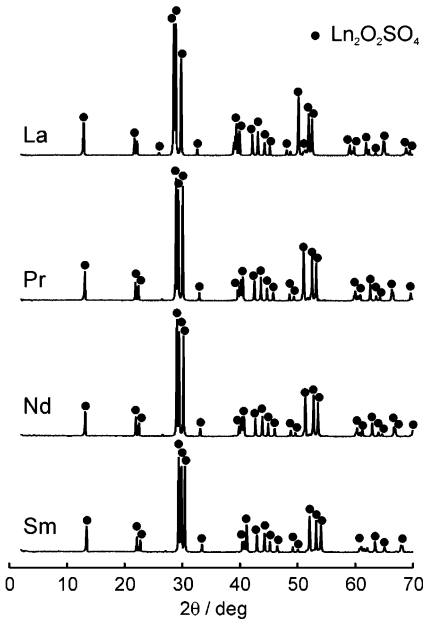

Figure 2. XRD patterns after calcining of $Ln_2(SO_4)_3 \cdot nH_2O$ (Ln = La, Pr, Nd, and Sm) at 900 °C in N_2.

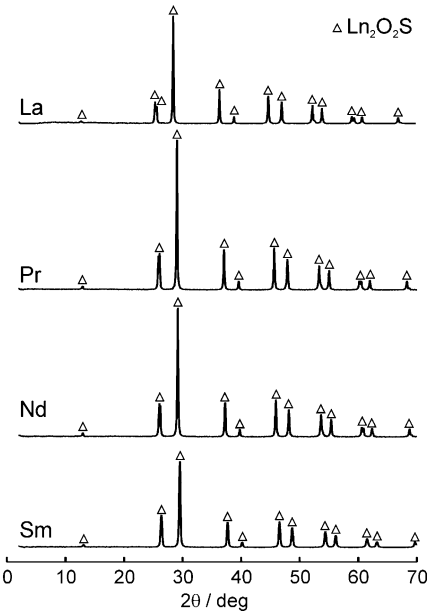

Figure 3. XRD patterns after calcining of $Ln_2O_2SO_4$ (Ln = La, Pr, Nd, and Sm) at 800 °C in H_2.

as-prepared $Ln_2O_2SO_4$ in a stream of H_2 at 800 °C. The $La_2O_2SO_4$ phase was converted into a single phase of oxysulfide, La_2O_2S, with a rhombohedral cell ($P3m1$),[17] which is isostructural with the corresponding La_2O_3. The same crystal structure was basically preserved for different Ln systems, but again, their lattice parameters *a* and *c* tend to decrease with the contraction of the Ln cations. The S/Ln atomic ratio for the samples appearing in Figures 1 and 2 was confirmed to be 0.5.

The crystal structures of oxysulfate and oxysulfide can commonly be described by alternative stacking of a $Ln_2O_2^{2+}$ layer and a layer of anion groups, i.e., sulfate (SO_4^{2-}) or sulfide (S^{2-}), as shown in Figure 4. The $Ln_2O_2^{2+}$ layer in both structures consists of LnO_4 tetrahedra linked together

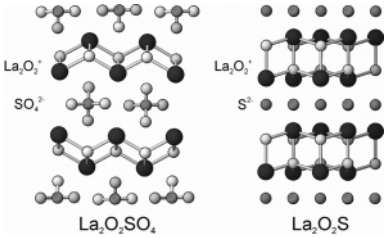

Figure 4. Crystal structure of $La_2O_2SO_4$ and La_2O_2S.

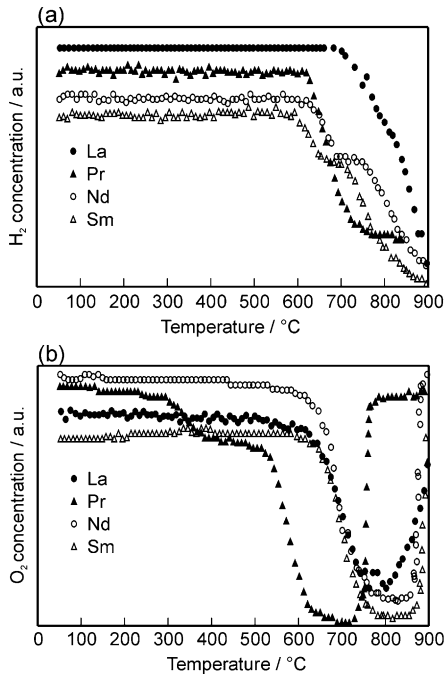

Figure 5. (a) TPR and (b) TPRO profiles of $Ln_2O_2SO_4$ in a flow of 10% H_2/He and 5% O_2/He, respectively. Heating rate 10 °C·min^{-1}.

by sharing of edges.[14] Every sulfate oxygen in $Ln_2O_2SO_4$ is coordinated with two Ln atoms. Thus, the phase transformation from $Ln_2O_2SO_4$ to Ln_2O_2S can be approximated as removal of oxide ions surrounding sulfur as a result of the reduction. Such a structural similarity between $Ln_2O_2SO_4$ and Ln_2O_2S is believed to be one important factor to attain reversible reduction/oxidation cycles of the present materials as described below.

The reduction behavior of several $Ln_2O_2SO_4$ phases was evaluated by TPR, which was carried out in a conventional flow system by heating at a rate of 10 °C·min^{-1} in a stream of 10% H_2/He. As shown in the TPR profiles in Figure 5a, the consumption of H_2 over $La_2O_2SO_4$ started at ca. 680 °C and required at least 1 h to be completed at 900 °C. After completion of H_2 consumption, the oxysulfate turned into oxysulfide (La_2O_2S). The oxysulfide thus formed was next subjected to TPRO measurement in a stream of 5% O_2/He as shown in Figure 5b. For Ln = La, oxygen consumption started at ca. 500 °C, giving rise to a peak at ca. 800 °C. After completion of the reoxidation, a single phase of $La_2O_2SO_4$ was restored as evident from the XRD pattern. The cumulative consumptions of H_2 and O_2 in the TPR/TPRO measurements were estimated to be 3.9 and 1.9 mol·mol^{-1}, respectively, supporting the occurrence of the stoichiometric reaction between $Ln_2O_2SO_4$ and Ln_2O_2S.

Here, it should be noted that the TPR/TPRO profiles are dependent on Ln. Among Ln = La, Pr, Nd, and Sm, the La

(17) Zachariasen, W. H. *Acta Crystallogr.* **1949**, *2*, 60.

system is more difficult to reduce than the others. For the reoxidation process, the Pr system exhibited an exceptional behavior. The onset of the main reoxidation peak for Ln = Pr was observed at a low temperature of ca. 500 °C, compared to >ca. 600 °C required for the other systems. In addition, a slow oxygen consumption was observed only for the Pr system at a lower temperature of ≥300 °C. The characteristic redox property of the Pr system may be related to the presence of a higher oxidation state of 4+, which was detected by XPS measurement, but the mechanism is not clearly understood at this stage.

These results give evidence that oxygen storage in the present system is accompanied by the redox of sulfur between oxidation numbers 6+ (SO_4^{2-}) and 2− (S^{2-}). This corresponds to a maximal storage capacity of 2 (mol of O_2)·mol^{-1}. It is very interesting that the present system utilizes the redox of sulfur in contrast to the conventional oxygen storage, which is due to the redox of metallic ions. The storage capacity of metal oxide systems should generally be limited to less than 0.5 (mol of O_2)·mol^{-1}, because in many cases the change of oxidation numbers does not exceed 2. By contrast, the present result implies the possibility of a much larger capacity for solid materials containing sulfur redox sites. Such a large-capacity oxygen storage by reversible redox of sulfur is only attained by oxysulfates/oxysulfides of lanthanide metals, because the formation of a thermally stable oxysulfate is not allowed in any other system. Sulfates of alkali metals cannot be used due to low melting points. Sulfates of alkaline-earth metals possess thermal stability higher than that of the lanthanide oxysulfates, but their reduction to sulfides is difficult at <1000 °C. Other sulfates containing p- and d-block metals were easily decomposed to evolve SO_2/O_2 at relatively low temperatures (<800 °C).

One drawback of the present oxygen storage material is the high operation temperature. The conventional CeO_2-ZrO_2 system can work at lower temperatures, <400 °C,[4−8] compared to >700 °C required for the present system. To reduce the temperatures for oxygen release as well as storage of $La_2O_2SO_4/La_2O_2S$, impregnation of noble metals was found to be effective in our previous report.[11] It is also well-known that oxygen storage over CeO_2-ZrO_2 can be promoted in the presence of impregnated Pt catalysts. In the case of $La_2O_2SO_4$, Pd can promote the reduction process more than Pt. Figure 6 exhibits the effect of impregnated Pd (1 wt %) on TPR and TPRO profiles of four different $Ln_2O_2SO_4$ systems. As can be judged from the comparison with Figure 5, the temperatures for the consumption of H_2/O_2 became lower in the presence of Pd. The effect implies that spillover of hydrogen and oxygen from the metal particles onto the $Ln_2O_2SO_4/Ln_2O_2S$ surface accelerates reduction and reoxidation, respectively. It has been suggested that the reduction of several metal oxides is facilitated by spillover of hydrogen, because of the higher reactivity of atomic hydrogen compared to molecular hydrogen.[18] The effect was dependent on the loading of Pd; i.e., the onset temperature of reduction/reoxidation decreased with an increase of Pd loading from 0 to 1 wt %.

(18) Sermon, P. A.; Bond, G. C. *Catal. Rev.* **1973**, *8*, 211.

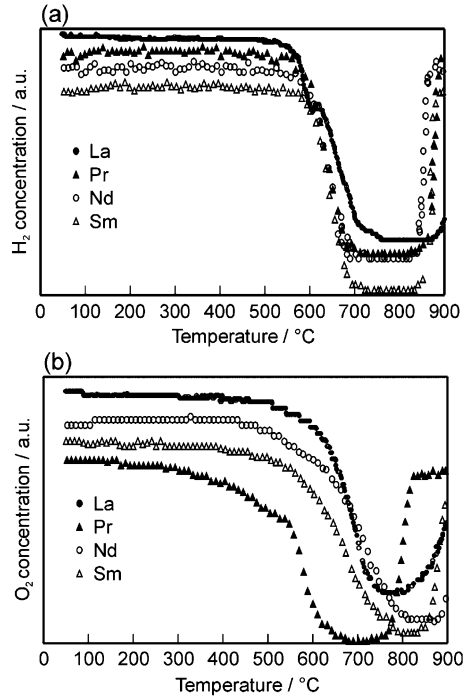

Figure 6. (a) TPR and (b) TPRO profiles of 1 wt % $Pd/Ln_2O_2SO_4$ in a flow of 10% H_2/He and 5% O_2/He, respectively. Heating rate 10 °C·min^{-1}.

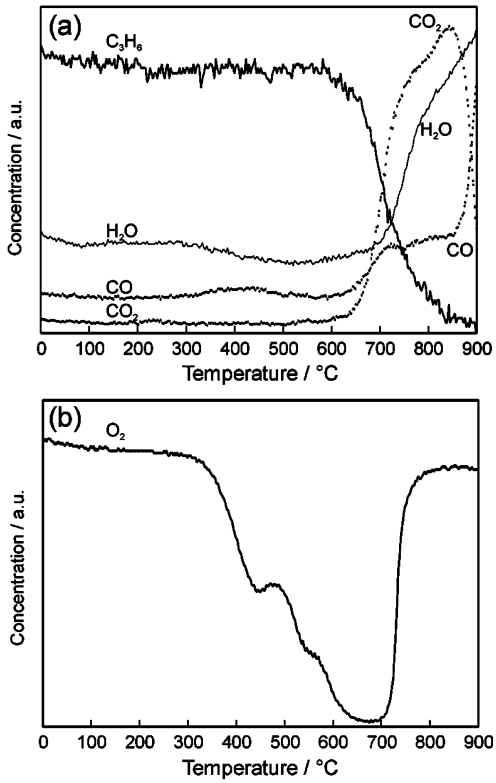

Figure 7. (a) TPR and (b) TPRO profiles of 1 wt % $Pd/Pr_2O_2SO_4$ in a flow of 1% C_3H_6/He and 5% O_2/He, respectively. Heating rate 10 °C·min^{-1}.

The oxygen storage materials should be capable of efficiently oxidizing not only hydrogen but also hydrocarbons to CO_2 and H_2O. In this regard, TPR by using C_3H_6 in place of H_2 would provide useful information on the reactivity of the present system. Figure 7 exhibits the effluent gas species versus the temperature ramp. The onset temperature of reduction was as high as for the H_2 TPR (Figure 6). As a primary product, CO_2 and H_2O were formed above 600 °C,

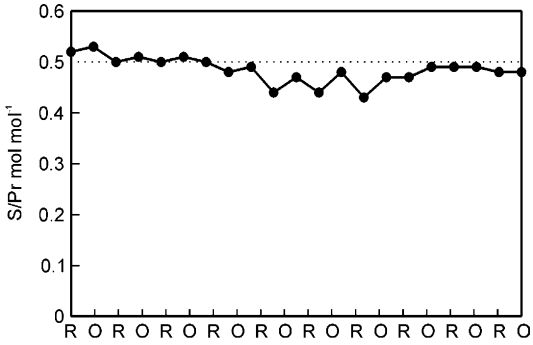

Figure 8. Change in the S/Pr ratio of 1 wt % $Pd/Pr_2O_2SO_4$ during cyclic redox treatment: R, reduction in H_2 at 700 °C for 1 h; O, reoxidation in air at 800 °C for 1 h.

whereas only a small amount of CO was observed at ≤850 °C, suggesting the occurrence of nonaerobic oxidation of hydrocarbon. When the TPR experiment was carried out in the absence of Pd, the consumption of C_3H_6 as well as the CO_2 yield became extremely small up to 900 °C. This is indicative of catalytic oxidation of C_3H_6 over Pd by oxygen originated from the oxysulfate solid. The reoxidation in this case took place at a much lower temperature of ca. 350 °C, compared to that of $Pd/Pr_2O_2SO_4$ after reduction by H_2.

To use the present system as an oxygen storage material, the stability in redox cycles is a very important factor. As described before, the thermal stability of the Pr system is less than that of the La system. Thus, one may consider the loss of sulfur due to vaporization in the redox cycles. The X-ray fluorescence analysis of the solid sulfur content was conducted after reduction in a stream of H_2 at 700 °C for 1 h and subsequent reoxidation in a stream of O_2 at 800 °C for 1 h were repeated. As shown in Figure 8, the ratio of S to Pr of 1 wt % $Pd/Pr_2O_2SO_4$ was kept constant at ca. 0.5 during 10 cycles of the redox treatment. Considering the H_2/O_2 flow rates in these treatments, the concentration of H_2S/SO_2 in the gas effluent should be <10 ppm. No precipitation of praseodymium oxides was detected by XRD after the redox cycles. With these results taken into consideration, the release of H_2S/SO_2 must be negligible.

For many sulfide materials, instability in the presence of water vapor is expected at elevated temperatures, because the reaction with water would form oxides and remove sulfur from solids. To check this stability, Pd/Pr_2O_2S was treated in a stream of 10% H_2O balanced by He at 800 °C. However, no change was observed in the XRD pattern and S/Pr ratio. The treatment in a stream of 10% H_2O and 10% O_2 balanced by He at 800 °C converted Pr_2O_2S to $Pr_2O_2SO_4$ as in the absence of H_2O. Also, it was confirmed that a $Pr_2O_2SO_4$ phase was stable and no adsorption of SO_2 was observed in a gas stream containing SO_2 at 400−800 °C. The present system is therefore expected to work stably even in the presence of SO_2. This feature may be important, because the conventional CeO_2-ZrO_2 adsorbs much of the SO_2 in an oxidizing atmosphere and the accumulated SO_2 is released as noxious H_2S when it turns to a reducing atmosphere.

It is well-known that the real oxygen storage performance should be evaluated under oscillating feed stream conditions,[19,20] where reducing and oxidizing atmospheres are cycled, because the rate of phase transformation is not considered under the stationary redox treatment as shown in Figure 8. Thus, we have studied the dynamic redox behavior of 1 wt % $Pd/Pr_2O_2SO_4$ by the use of a flow microbalance. The representative result of oxygen release/storage cycles at 700 °C is exhibited in Figure 9, in comparison with the result of a CeO_2-ZrO_2 material, where nearly invariant weights were reached on each atmosphere. On approaching a constant weight in flowing N_2 at 700 °C, the gas feed was switched to a mixture of 5% H_2 in N_2. This gave rise to a steep weight loss of 15%, which corresponds to the stoichiometric reduction of $Pr_2O_2SO_4$ to Pr_2O_2S. A subsequent switch to a mixture of 20% O_2 in N_2 immediately caused a weight gain as was observed before the reduction, accompanied by a sharp exothermic peak. Following this first redox period, the gas feed was switched every 30 min between mixtures of 20% O_2 and 5% H_2 in N_2, yielding almost reversible cyclic change of the sample weight. The cyclic oxygen storage/release experiment demonstrated very clearly that the present oxygen storage capacity was ca. 8 times larger than that of CeO_2-ZrO_2 at 700 °C. Higher performance is also evidenced by comparing the rate of oxygen release and storage as shown in Table 1, which is determined from the slope of the weight change in Figure 9. The different rates between oxygen release and storage are consistent with the result of the TPR/TPRO experiment (Figure 6). The oxygen release/storage cycles between Pr_2O_2-

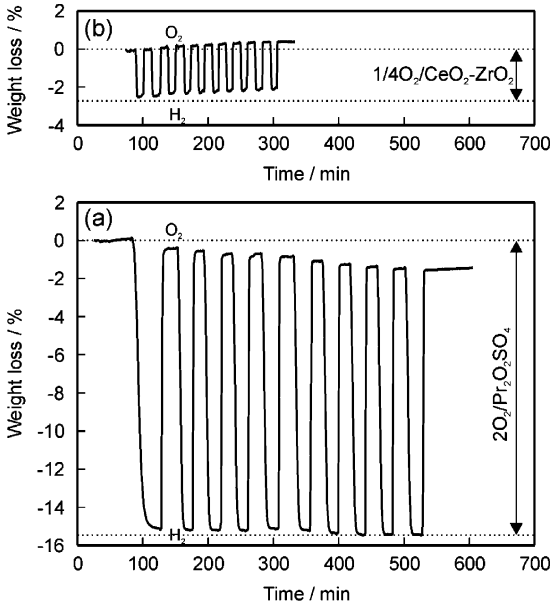

Figure 9. Reduction−reoxidation cycles at 700 °C over (a) 1 wt % $Pd/Pr_2O_2SO_4$ and (b) 1 wt % Pt/CeO_2-ZrO_2 in a microbalance. A mixture of 5% H_2 in He was used for reduction, and a mixture of 20% O_2 in He was used for oxidation.

Table 1. Rate of Oxygen Release and Storage for 1 wt % $Pd/Pr_2O_2SO_4$ and 1 wt % Pt/CeO_2-ZrO_2

	1 wt % $Pd/Pr_2O_2SO_4$	1 wt % Pt/CeO_2-ZrO_2
oxygen release/(mol of O_2)·mol^{-1}·min^{-1} (reduction)	0.18	0.092
oxygen storage/(mol of O_2)·mol^{-1}·min^1 (reoxidation)	1.01	0.32

(19) Holmgren, A.; Andersson, B. *J. Catal.* **1998**, *178*, 14.
(20) Boaro, M.; de Leitenburg, C.; Dolcetti, G., Trovarelli, A. *J. Catal.* **2000**, *193*, 338.

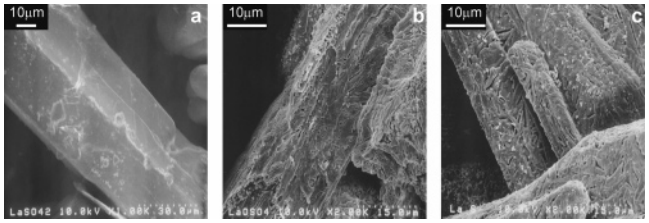

Figure 10. SEM images of (a) $La_2(SO_4)_3$, (b) $La_2O_2SO_4$, and (c) La_2O_2S.

SO_4 and Pr_2O_2S can proceed 2 or 3 times faster than that for CeO_2-ZrO_2 when the temperature is high enough for the redox of sulfur. This is a very interesting feature considering that Pt/CeO_2-ZrO_2 can work at much lower temperatures.

Due to high operation temperatures, textural stability is of crucial importance for the present oxygen storage system. Microstructural change during transformation from sulfate to oxysulfate and oxysulfide was observed by FE-SEM as shown in Figure 10. The sulfate $La_2(SO_4)_3$ consisted of nonporous columnar crystals with a smooth surface after dehydration at 500 °C. The oxysulfate $La_2O_2SO_4$ exhibited a similar external morphology, but the interior exhibited a highly porous texture, which is formed by skeletonization probably due to the elimination of SO_2/O_2. A similar porous texture was preserved for the oxysulfide La_2O_2S, but the pore size appears to increase. Accompanied by such a microstructural change, the surface area increased from <1 m^2 g^{-1} ($La_2(SO_4)_3$) to 22 m^2 g^{-1} ($La_2O_2SO_4$) and 19 m^2 g^{-1} (La_2O_2S).

Figure 11a shows the N_2 adsorption−desorption isotherms of $La_2O_2SO_4$, and Ln_2O_2S measured at 77 K. In contrast to the nonporous nature of $La_2(SO_4)_3$, the isotherms of $La_2O_2SO_4$ and La_2O_2S were very similar to IUPAC type III, which was flat up to a relative pressure of ca. 0.8 and then sharply increased near the saturation of vapor pressure. This is indicative of the absence of micropores and mesopores, but significant formation of macropores after decomposition of $La_2(SO_4)_3$. The pore size distribution calculated from the adsorption isotherms (Figure 11b) presents peak maxima at pore radii of ca. 20 and 45 nm for $La_2O_2SO_4$ and La_2O_2S, respectively. Although macropores of more than 100 nm are visible in the SEM images (Figure 10), the result implies that the pore size of $La_2O_2SO_4$ is increased by the reduction to La_2O_2S due to the removal of 4 mol of oxide ions from the structure. Formation of such a porous texture is believed be significantly effective in facilitating the gas diffusion and solid−gas reactions in the redox cycles. No textural change was observed after reduction at 700 °C and subsequent reoxidation at 900 °C were repeated for 10 cycles. The textural stability is therefore enough for the high-temperature operation.

In summary, we have found a novel oxygen storage material, lanthanide oxysulfate/oxysulfide, which utilizes

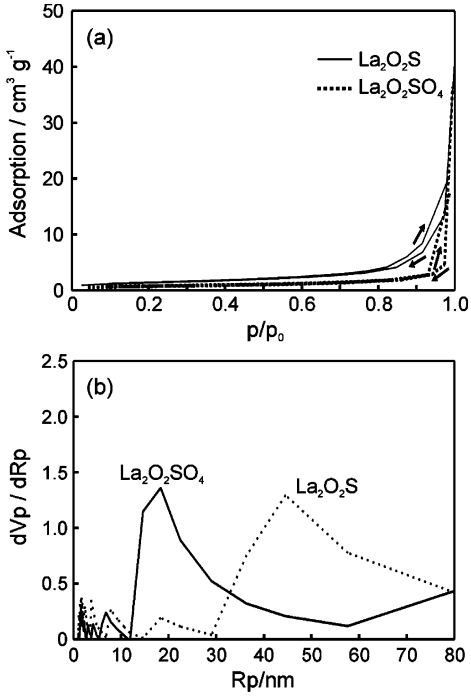

Figure 11. (a) N_2 adsorption isotherms at 77 K and (b) pore size distribution of $La_2O_2SO_4$ and La_2O_2S.

sulfur in the metal oxide matrix as a redox center. This is completely in contrast to the conventional oxygen storage based on the redox of metal cations. Thermally stable lanthanide oxysulfate/oxysulfide systems with Ln = La, Pr, Nd, and Sm exhibited a large storage capacity of 2 (mol of O_2)·mol^{-1}, which required higher operation temperatures (≥600 °C) compared to CeO_2-ZrO_2. The reversible redox is allowed by common structural units of oxysulfate and oxysulfide, which consist of alternative stacking of $Ln_2O_2^{2-}$ and positive divalent layers, SO_4^{2-} or S^{2-}. Among the four Ln systems, the redox of $Pr_2O_2SO_4/Pr_2O_2S$ takes place at the lowest temperature. Moreover, the redox cycles can be facilitated by impregnating Pd because the spillover can supply active oxygen as well as hydrogen species onto the surface of oxysulfate/oxysulfide. The oxygen release and storage are faster than those of CeO_2-ZrO_2, when the temperature is high enough for the redox of sulfur (≥700 °C). One promising microstructural feature adequate for the oxygen storage/release is the porous texture, which is formed spontaneously when a mixture of SO_2/O_2 is eliminated from the nonporous sulfate crystals.

Acknowledgment. We acknowledge the financial support provided by a Grant-in aid for Scientific Research from the Ministry of Education, Science, Sports, and Culture, Japan.

CM0479640